

Synthesis a New Magnetic Nanoparticles and Study the Interaction with Xanthine Oxidase

Hussain Kadhem Al-Hakeim^{1,*}, Mustafa M. Kareem¹, Eric A. Grulke²

¹Department of Chemistry- faculty of Science-Kufa University, Iraq

²Department of Chemical and Material Engineering-Engineering Faculty-Kentucky University

*Corresponding author: headm2010@yahoo.com

Received October 01, 2014; Revised October 15, 2014; Accepted October 22, 2014

Abstract Two new magnetic nanoparticles (MNPs) were prepared using magnetic iron oxides with cholesterol and sulphadiazine. These compounds were prepared by coprecipitation methods of the iron oxide (II and III) and then the prepared MNP were incubated with the cholesterol and sulphadiazine. The synthesized compounds were identified using many techniques including TEM, SEM, DLS, and TGA. The results showed the formation of new magnetic nanoparticles; MNP@Cholesterol and MNP@Sulphadiazine. The interaction between the prepared MNPs and xanthine oxidase (XO) was studied as a potential method for the inhibition of its activity, for the extraction of XO from biological fluids or for the immobilization of XO on the surfaces of MNPs. The interaction studies involve incubation of XO solution with the suspension of the prepared MNPs using different concentration of XO solutions and fixed weights of MNPs. Adsorption studies of XO on MNPs showed that the prepared MNPs have the ability to extract suitable amounts of XO from solution. Circular dichroism study of the adsorption of XO on the prepared MNPs showed a significant changes in the secondary structures, namely reduction of the α -helix structure. Furthermore, fluorospectrophotometric study showed changes in the tertiary structure of the XO due to the interaction with the active sites of the prepared MNPs. Kinetic study of the inhibition of XO activity by the prepared MNPs showed a mixed inhibition due to the changes in the original XO enzyme after the interaction with the surfaces. Magnetic Fe₃O₄ showed the higher inhibition activity followed by MNP@Sulphadiazine and MNP@Cholesterol-XO, respectively.

Keywords: magnetic nanoparticles, surface modification, protein adsorption, Xanthine Oxidase, and enzyme inhibitor

Cite This Article: Hussain Kadhem Al-Hakeim, Mustafa M. Kareem, and Eric A. Grulke, "Synthesis a New Magnetic Nanoparticles and Study the Interaction with Xanthine Oxidase." *American Journal of Nanomaterials*, vol. 2, no. 2 (2014): 13-20. doi: 10.12691/ajn-2-2-1.

1. Introduction

Nanoparticles (NPs) are of great scientific interest as they are, in effect, a bridge between bulk materials and atomic or molecular structures. NPs have unique properties that may be useful in a diverse range of applications, and consequently they have attracted significant interest. The interesting and unexpected properties of NPs are largely due to the large surface area of the material, which governs the contributions made by the small bulk of the material [1].

Iron oxide magnetic nanoparticles (MNPs) have attracted much attention due to their fine magnetic properties and massive fields of applications in modern science. Medical and biochemical applications of MNPs involve drug delivery [2], gene delivery [3], protein separation [4], magnetic resonance imaging [5], treatment by hyperthermia [5]. The magnetic properties strongly depend on their synthesis method and their surface characterization [8]. Surface coating with some molecules may enhance or reduce the ability of MNPs to interact

with other molecules [9]. Therefore, synthesis of new MNPs with various surface properties is still an interesting field of study.

The protein-nanoparticle interactions involves the formation of a dynamic layer of proteins or other biomolecules adsorbed on the nanoparticle surfaces called "corona" [10]. Interaction of NPs with proteins and the formation of corona affect the physicochemical properties of both biomolecules and the NPs and considered as the basis of NPs bioreactivity [11]. It is appear that highly selective protein adsorption, added to the fact that particles can reach subcellular locations, results in significant new potential impacts for NPs on protein interactions and cellular behavior. The protein corona may influence cellular uptake, inflammation, accumulation, degradation and clearance of the NPs. Furthermore, the NPs surface can induce conformational changes in adsorbed protein molecules which may affect the overall bio-reactivity of the nanoparticle [12]. Among these bioactivity processes, enzyme inhibition by NPs is an important issue for study as some drugs, in fact, are enzyme inhibitors [13]. One of these enzymes that are targeted by inhibitors is xanthine oxidase (XO). It plays an

important role in the catabolism of purines. XO catalyzes the formation of xanthine which can further catalyze the oxidation of xanthine to uric acid. Accumulation of uric acid can result in hyperuricaemia, leading to arthritis and gout [14]. The search for XO inhibitors is still an interesting field for study [15,16]. The present study aimed to prepare new magnetic NPs by direct surface modification of the original magnetic Fe₃O₄ NPs using sulphadiazine and cholesterol. The prepared MNPs will be used to immobilize XO enzyme on their surfaces and study the possible changes in enzyme activity and secondary and tertiary structures induced by the MNPs for future medical applications.

2. Materials and Method

2.1. Synthesis of the New Magnetic Nanoparticles

Iron Oxide nanoparticles Fe₃O₄

In the present work Fe₃O₄ nanoparticles were prepared by a modified co-precipitation method [17]. Briefly, 0.04 mol of FeCl₃·6H₂O and 0.02 mol of FeSO₄·7H₂O were dissolved in 50 ml of 0.5 M HCl solution. Then, 500 ml of 1.5 M NaOH was added dropwise to the solution under vigorous stirring at 80 °C. The Fe₃O₄ precipitate obtained was separated using a magnet and was repeatedly washed with deionized water until the supernatant becomes neutral. Finally, the precipitate was dried at 50 °C for 4h and then overnight at room temperature. For the preparation of MNP@Cholesterol or MNP@Sulphadiazine, same method was followed but before the separation of the obtained Fe₃O₄, a volume of oversaturated solution of cholesterol or folic acid at ratio 2:1 was added to MNPs suspension with continuous stirring at 80 °C for 1h. Then, the suspensions were transferred to a watch glass and placed in an oven at 40 °C overnight until completely dried. Transmission electron microscopy (TEM) was used to visualize the morphology and size of the prepared MNPs.

2.2. Estimation of Xanthine Oxidase Activity

XO from buttermilk has a molecular weight of 275,000D was used in all the enzyme containing experiments. The enzyme activity was measured using Kalckar method [18] as follows: into a quartz cuvette pipette 2.9 ml of different concentration of xanthine (substrate) solution (0.01, 0.02, 0.03, 0.04, 0.05, 0.06, 0.07 and 0.08 mM). After zero adjustment at 290 nm, One hundred microliters of enzyme solution (0.1 U per ml of 0.05 M Sodium phosphate buffer) were added to the cuvette, mixed and the increase in absorbance at 290 nm was recorded during 5 minutes. The increase in absorbance at 290 nm, caused by the oxidation of xanthine to uric acid, is a measure of the catalytic activity of XO.

2.3. Estimation of Kinetic Parameters

Kinetic parameters K_m, V_{max} were calculated from the Lineweaver-Burke equation ($1/v_0 = (K_m/V_{max}[S]) + 1/V_{max}$) by plotting $1/v_0$ vs. $1/[S]$. Where; v_0 : initial velocity $\mu\text{M}/\text{min}$, V_{max}: maximum velocity $\mu\text{M}/\text{min}$, K_m: Michaelis

constant (μM), S: substrate concentration (μM). Then intercept = $1/V_{max}$ and slope = K_m/V_{max} .

2.4. Interaction of Xanthine Oxidase with Magnetic Nanoparticles

Two mg/mL of the prepared magnetic nanoparticles (MNP, MNP@cholesterol, and MNP@sulfadiazine) were ultrasonicated for 20 minutes then cooled. The following concentration of XO enzyme were prepared in phosphate buffer: 0.2, 0.4, 0.6, 0.8, 1, 1.4 and 1.6 U/ml. Two and a half milliliters of the MNPs solution were mixed with 2.5 ml of XO solution. The mixture was mixed for 60 minutes at room temperature (22–25 °C). The mixture then was centrifuged at (7,500rpm) for 25 minutes at 20 °C and the supernatant then separated. The concentration of XO (as protein) was estimated spectrophotometrically using Barford's method at 595nm [19]. The isotherms were constructed between xanthine oxidase concentration at equilibrium (C_e) and amount of xanthine oxidase that adsorbed on the MNPs (Q_e). The isotherms were studied to find out the best adsorption isotherm that can explain the adsorption isotherm.

2.5. CD Spectra

CD spectra of free xanthine oxidase, XO-MNP@Cholesterol, and XO-MNP@Sulfadiazine composites after adsorption were obtained by using the following concentrations: 0.2 U/ml free xanthine oxidase, 50mM potassium phosphate, pH=7.5. The free XO were put in 0.1 cm Spectrosil quartz cuvette (Starna Cells) and the cuvette was put in the Jasco CD Spectrometer at 20 °C. Three scans were averaged by using Chirascan Pro-Data Viewer software. Equipment parameters consisted of a 20.0–99.0 °C gradient with stepped ramping, 10 °C per step, with a 60 s equilibration time, and a 20 s read at each step subsequent to equilibration. Ellipticity profiles were fitted to a two-state model.

2.6. Fluorescence Spectrophotometer

The instrument was adjusted to zero using phosphate buffer 50mM, then the spectra of free xanthine oxidase solution (0.1U/ml) was measured, also the spectra of XO-MNPs, XO-MNP@cholesterol, and XO-MNP@sulfadiazine-XO were measured.

3. Result and Discussion

3.1. Characterization MNPs by TEM

The size and morphology of the synthesized magnetic nanoparticles were confirmed via TEM, which demonstrates the shape varies from spherical to cubic or truncated cubic (octahedral) structures for large particles with broad size distribution (20–100 nm). The formed MNP were ball shape, as shown in Figure 1.

The images showed that the MNP-Cholesterol & MNP-Sulfadiazine are larger than the MNPs and the larger size leads to transformation in the shape from small ball shape into larger cubic shape [20,21]. Furthermore, the (Cholesterol & Sulfadiazine) layers appear as lighter than the cubic core of magnetic nanoparticles indicating the formation of new nanoparticles.

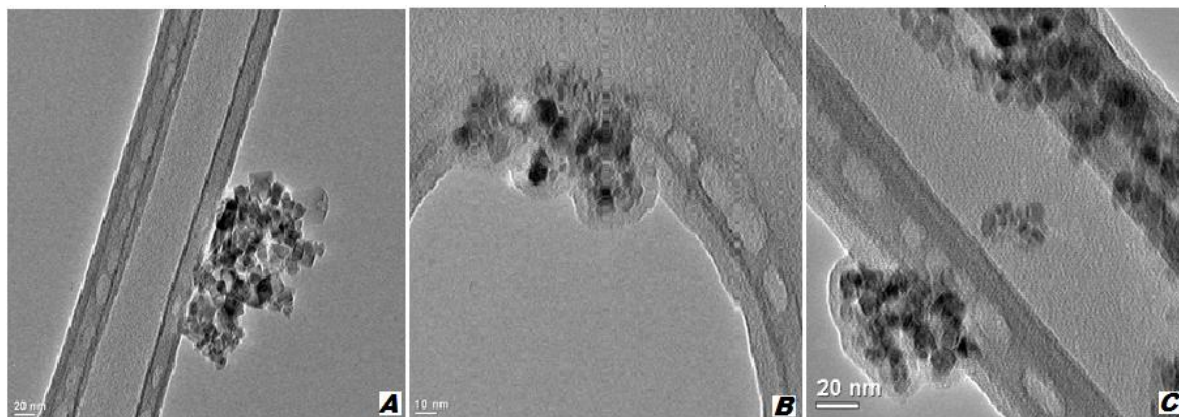


Figure 1. TEM images of the prepared MNP under very high resolution A-MNP, B-MNP@Cholesterol and C-MNP@Sulphadiazine

3.2. Thermogravimetric Analysis

According to TGA plots that presented the weight loss percentage per degree of MNPs plotted versus the increase in temperature as in [Figure 2](#). It is clear that the most weight loss percentages occur at 100 °C, due to loss of water that bound weakly to the structure of NPs. There is a gradual increase in the weight loss percentage as temperature increases due to loss of water that tightly bound to the structure of the MNP. The weight loss from MNP@Cholesterol and MNP@Sulphadiazine occurs at

lower temperature than the original MNPs. This results indicating the higher adsorption of water for the two new NPs than the free MNPs. The change in surface properties is expected after coating with cholesterol and sulphadiazine. Availability of various functional groups including hydrophilic and hydrophobic groups coating the surface of MNPs should affect the physicochemical properties of the surface including its ability to adsorb or absorb water molecules [22].

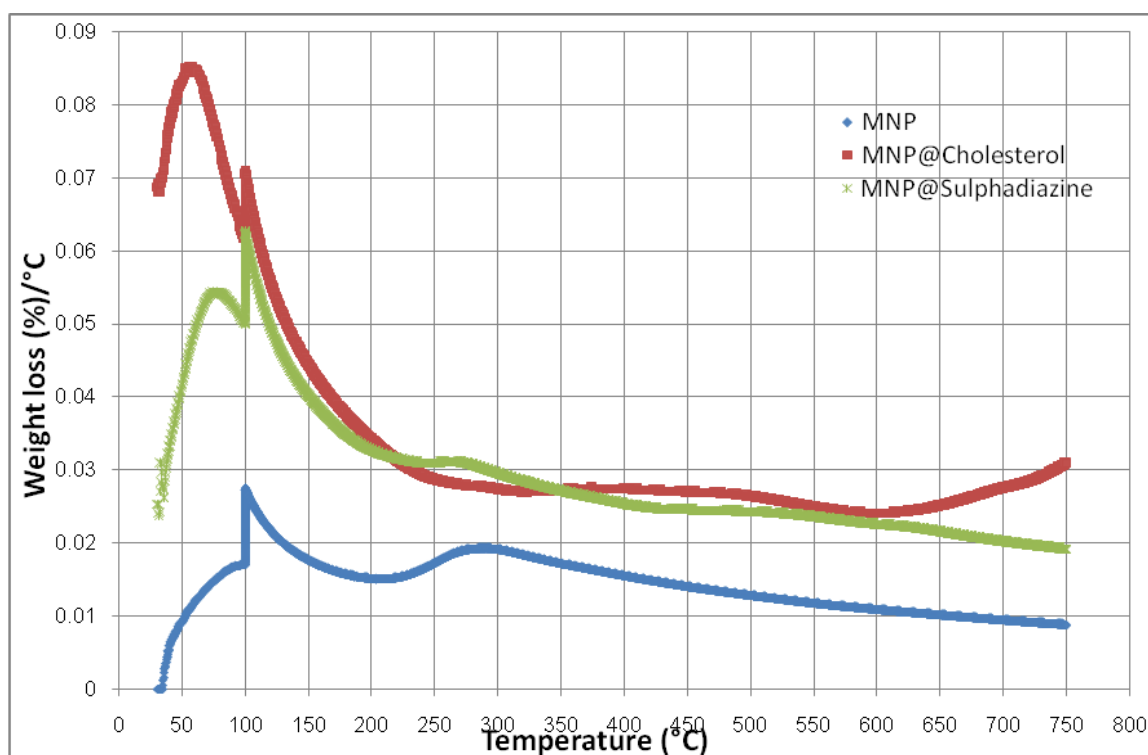


Figure 2. Weight loss percentage per degree of MNP as a function of increasing temperature

3.3. Properties of NP after interaction with Xanthine Oxidase

After adsorption of XO's on the MNPs, MNP@Cholesterol, and MNP@Sulphadiazine, the formed composites were separated and visualized by TEM. [Figure 3](#) showed the TEM images of the composites of XO's with MNPs, MNP@Cholesterol, and MNP@Sulphadiazine, respectively. These images showed cubic particles larger

than the original (uncoated) particles surrounded by a lighter layer of the protein corona.

Much research showed that the interaction between proteins and NPs surface leads to the formation of proteins "corona" around NPs that largely defines their biological identity as well their potential toxicity and other vital properties [23,24].

The proteins that readily occupy the NPs surface should either have high concentrations and high association rate

constants or have lower concentrations but a higher affinity [12]. However in the presence of one type of proteins in the solution in contact with NPs, the factors affecting the interaction properties include the protein characteristics such as electrostatic interactions, protein stability, and kinetic parameters in addition to the properties of the surface active sites. NPs have significant adsorption capacities due to their relatively large surface

area, therefore they are able to bind or carry other molecules such as chemical compounds, drugs, and proteins attached to the surface by covalent bonds or by adsorption. Hence, the physicochemical properties of NPs, such as charge and hydrophobicity, can be altered by attaching specific chemical compounds, peptides or proteins to the surface [25,26].

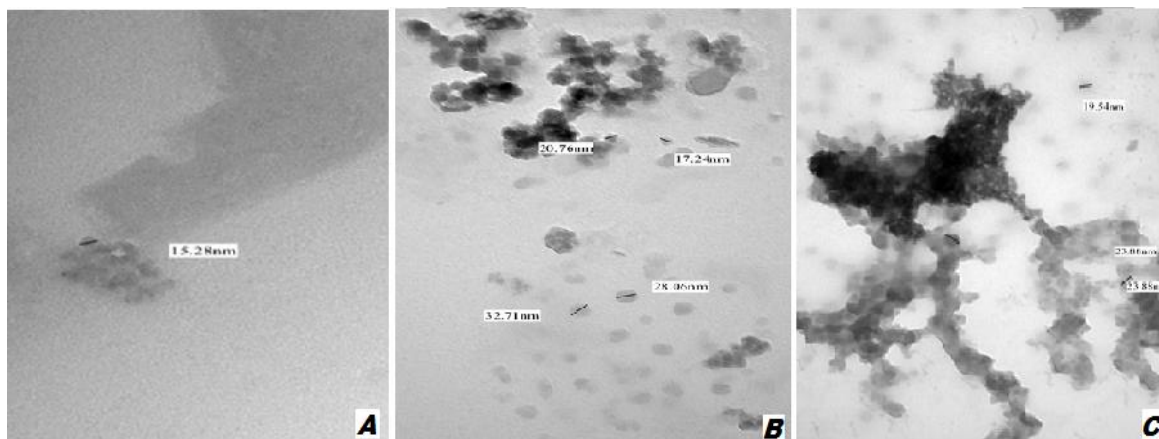


Figure 3. A-Xanthine Oxidase-MNP composite B-MNP@Cholesterol-XO composite and C-MNP@ Sulfadiazine-XO composite

3.4. CD Spectra

The changes in the secondary structure of xanthine oxidase after adsorption on MNP's was analyzed via CD spectroscopy, which is particularly efficient in determining the protein folding and in characterizing the secondary structure of protein and denaturant stabilities

[27]. The secondary structure can be determined via CD spectroscopy in the far-UV spectral region (200–260 nm), and the chromophore at this wavelength is the peptide bond. Figure 4 showed the CD diagrams of the XO adsorbed on MNPs, MNP@Cholesterol and MNP@Sulphadiazine, respectively in comparison with free enzyme.

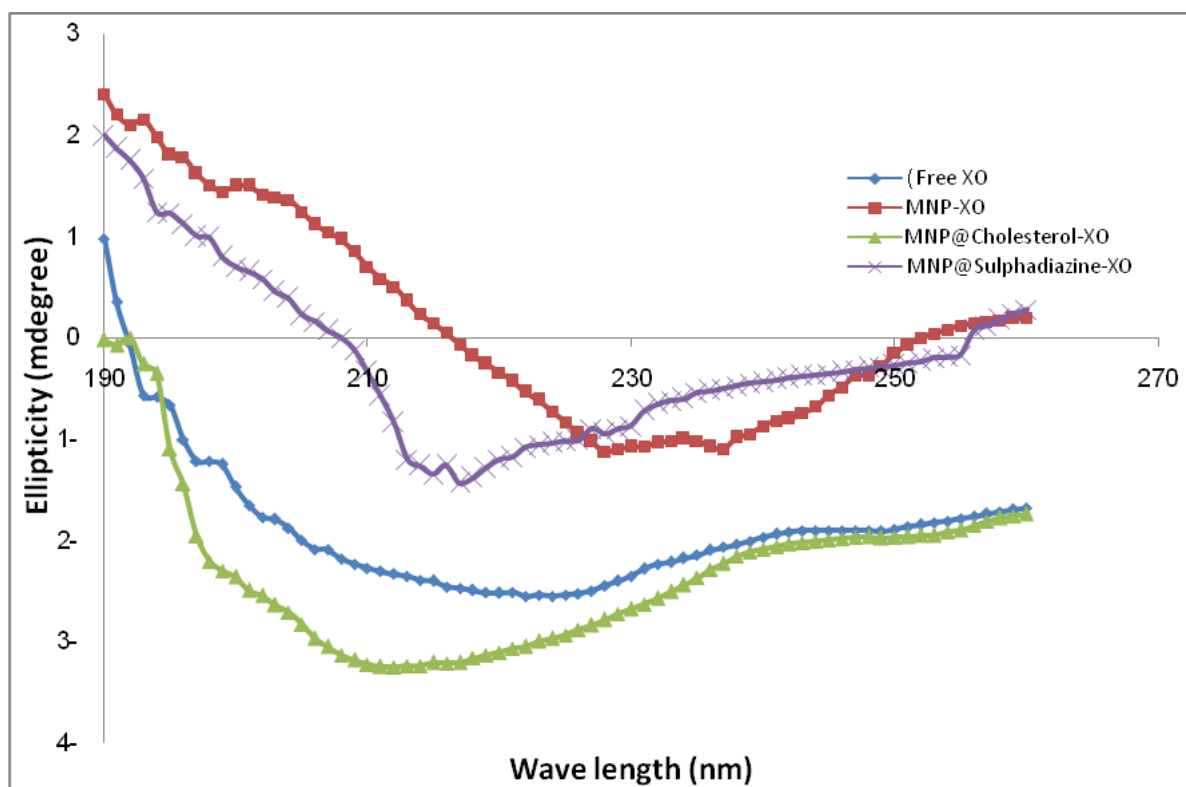


Figure 4. CD for the free XO, MNP-XO, MNP@Cholesterol- XO, MNP@Sulphadiazine-XO

The CD results were analyzed using the K2D3 web server to determine the change in the X secondary structure from the CD spectra according to the published

software [28]. The results of the analysis are presented in Table 1.

Table 1. The percentages of secondary protein structure components of free and immobilized XO enzyme.

Nanoparticle/Structure	α -Helix %	β -Sheet %	Random coil %
Free XO	37.62	11.41	50.97
MNP-XO	22.31	17.11	60.58
MNP@Cholesterol-XO	35.85	12.96	51.19
MNP@Sulphadiazine-XO	27.34	14.17	58.49

Conformational rearrangements in which the secondary and/or tertiary structure of the protein changes because of adsorption have been observed. These changes could even be a substantial driving force for adsorption. The significant change in the secondary structure indicates that the adsorption of XO on MNPs involves a contact with the domains rich in alpha structures on the XO molecule surface. The affected secondary structures depend on the change in orientation towards the surface active sites and the magnitude of the adsorption forces. In one study, it is found that the secondary structure of glucose oxidase (protein) is changed after adsorption on NP surface and maintain its native structure when adsorbed on other type of NP [29].

3.5. Fluorescence Spectroscopy

Fluorescence spectroscopy was used to monitor the changes in the tertiary structure of the protein. The three amino acids with intrinsic fluorescence properties are phenylalanine, tyrosine, and tryptophan. However, only tryptophan was used experimentally because the quantum yields (emitted photons/excited photons) of tryptophan are sufficiently high to achieve good fluorescence signal. Therefore, this technique is limited to the proteins with tryptophan. These residues can be used to follow the protein folding because fluorescence properties (quantum yields) are sensitive to the environment, which changes when the protein folds/unfolds [30].

The fluorescence emission of the free and adsorbed xanthine oxidase was determined from the spectra obtained using a carry eclipse fluorescence spectrophotometer. Figure 5 showed the spectra of fluorospectrophotometry of the XO adsorbed on MNPs, MNP@Cholesterol and MNP@Sulphadiazine, respectively in comparison with free enzyme.

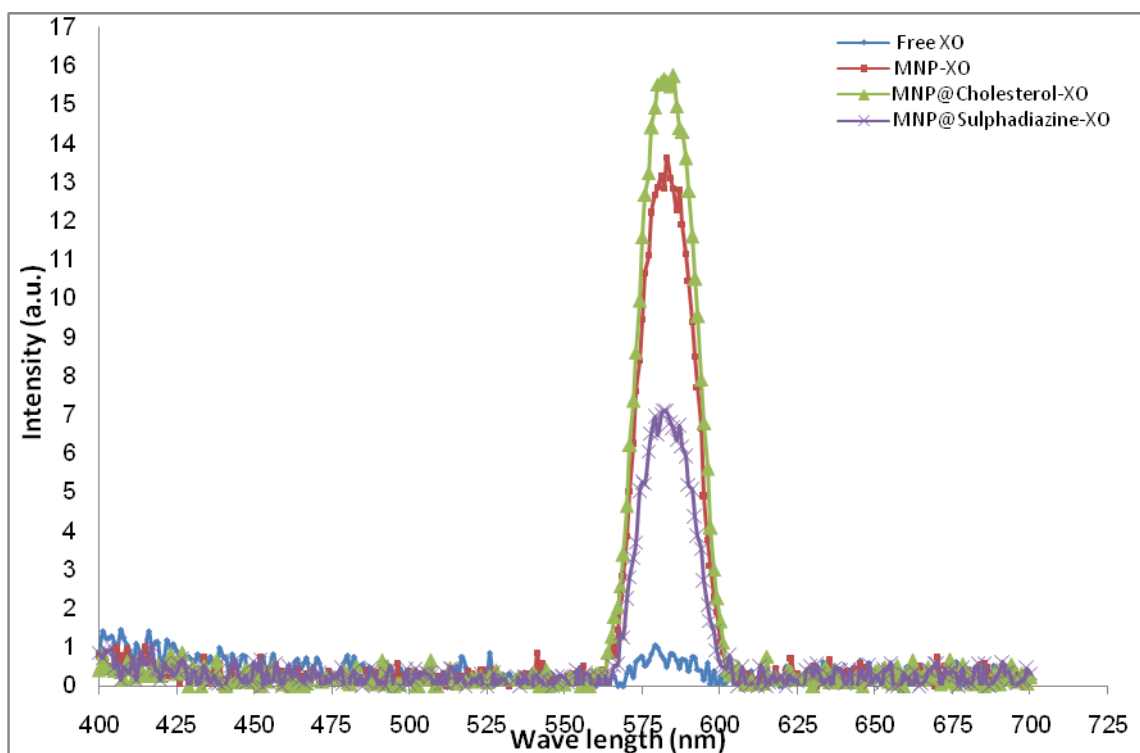


Figure 5. Fluorescence spectra of free XO, MNP-XO, MNP@Cholesterol-XO, and MNP@Sulphadiazine-XO

The change in the spectra may be due to the change in the environment polarity of the protein or the environment surrounding the tryptophan residues, which may be buried in the hydrophobic core of proteins; these changes result in a shift by 10 nm to 20 nm compared with those on the surface of the protein [31]. Figure 5 showed a significant changes in the tertiary structure of XO enzyme after adsorption on MNPs. The fluorescence emission of XO's residues (free and dispersion) were determined from spectra obtained on carry eclipse fluorescence spectrophotometer, a speed of scan 600 nm/min, the samples were emission at scanned from 290–400 nm at room temperature. Fluorescence emission for free XO's and dispersion XO's with MNP's was at (400 nm) [31]. Although tyrosine and phenylalanine are natural fluorophores in proteins,

tryptophan is the most extensively used amino acid for fluorescence analysis of proteins. In a protein containing all three fluorescent amino acids, observation of tyrosine and phenylalanine fluorescence is often complicated due to the interference by tryptophan by resonance energy transfer [32]. Fluorescence of phenylalanine is weak and seldom used in protein studies [32]. Hence, the term "natural protein fluorescence" is almost associated with tryptophan fluorescence.

3.6. Adsorption Process

In order to obtain a better description for the behavior of the XO's adsorption on the surfaces of the nanoparticles, the adsorption isotherm were constructed for the adsorption of XO's on MNPs, MNP@Cholesterol,

&MNP@Sulfadiazine Adsorption isotherm of XO enzyme on MNPs is presented in Figure 6.

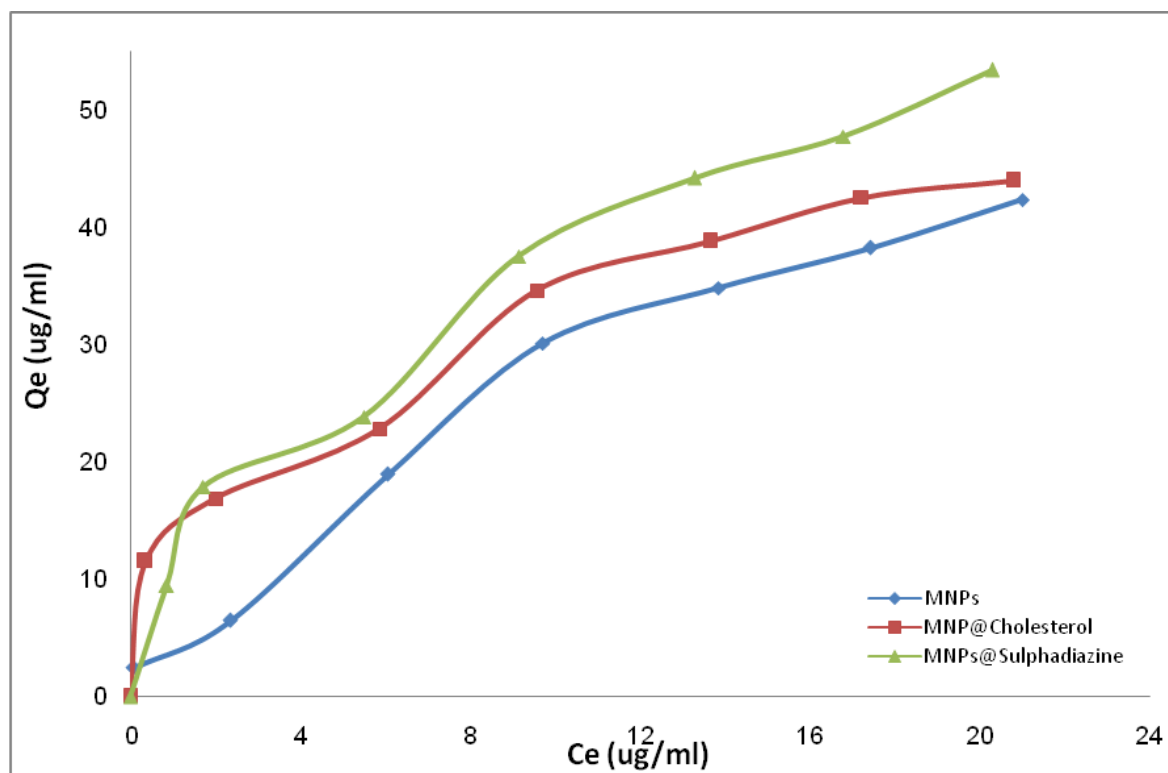


Figure 6. Adsorption isotherm of XO enzyme on MNPs, MNP@Cholesterol, and MNP@Sulphadiazine

Plotting C_e versus Q_e produce adsorption isotherm that is applied very well with the Sips equation as seen in the above figures. The Sips model for heterogeneous adsorption requires a parameter that describes the maximum adsorption amount Q_m (mg/g). The parameters could have been estimated as part of the fitting exercise, but we chose to estimate the parameters from the general shape of the molecule [33]. The heterogeneity factors of Sips equation, t & k , of the adsorption of xanthine oxidase on MNP's, MNP@Cholesterol-XO and MNP@Sulphadiazine-XO were ($t=0.623$, $K_s=0.159$), ($t=0.520$, $K_s=0.210$), and ($t=0.620$, $K_s=0.158$), respectively. The (t) value for the adsorption process of XO on MNPs are lower than one indicating that the adsorbed XO molecules interact with neighboring XO molecules in different forces. This mechanism appears to be consistent with a low XO adsorption at low solution concentrations, followed by rapid increases (lateral effect). The low K_s values for the adsorption processes suggest a small portion of the surface heterogeneity of magnetic nanoparticles [34]. The development of biocompatible nanomaterials for enhancing or modifying the bio-properties is an important challenge in the biotechnology field [35]. The protein adsorption laws and principles are applicable on XO's as a protein compounds. Proteins are not simply hard spherical colloidal particles. Because of this, several authors have considered changes in orientation, conformation and formation of two-dimensional structures to explain observed adsorption phenomena. Most proteins have a tertiary structure that is spheroidal with a major and minor axis, rather than spherical [36]. Hence, initial adsorption to a surface can occur in more than one orientation with respect to the surface. Subsequent transition in time from one orientation to the other is likely if a favorable higher contact area is created. When the concentration of bulk

protein is high, overshoots in the adsorbed amount, have been reported in the literature [37].

3.7. Enzyme Inhibition

The activity of the free XO enzyme and the enzyme immobilized on different types of magnetic nanoparticles was measured by using nine different concentrations of xanthine as a substrate and at human body temperature (37.5 °C). The Lineweaver-Burk plots of the three experiments were shown in Figure 7.

Kinetic parameters V_{max} and K_m were calculated from the regression equation of each line and presented in Table 2. The activity of the enzyme at the highest concentration of xanthine used in the experiments is also cited in the Table 2.

Table 2. V_{max} and K_m of the free XO enzyme, immobilized on MNPs, MNP@Cholesterol, and MNP@Sulphadiazine

Nanoparticle	Slope	Intercept	$V_{max}(U.min^{-1})$	K_m (mM)
Free XO	0.0190	0.1488	6.7204	0.1277
MNP@Cholesterol-XO	0.1029	0.1574	6.3532	0.6538
MNP@Sulphadiazine-XO	0.0917	0.1654	6.0460	0.5544
MNP-XO	0.0775	0.1685	5.9347	0.4599

The changes in the V_{max} and K_m indicated a mixed inhibition of the activity of the XO enzyme after interaction with magnetic NPs. These changes may be due to the changes in the secondary and tertiary structures of the enzyme as a result of the interaction between the XO molecule with the active sites on the NPS. Proteins are flexible molecules that undergo conformational changes as part of their interactions with other proteins or drug molecules [38]. Many proteins undergo changes in their structure during biochemical processes such as binding and transport. Such conformational changes are crucial to

the functioning of proteins, and by extension, to most biological processes.

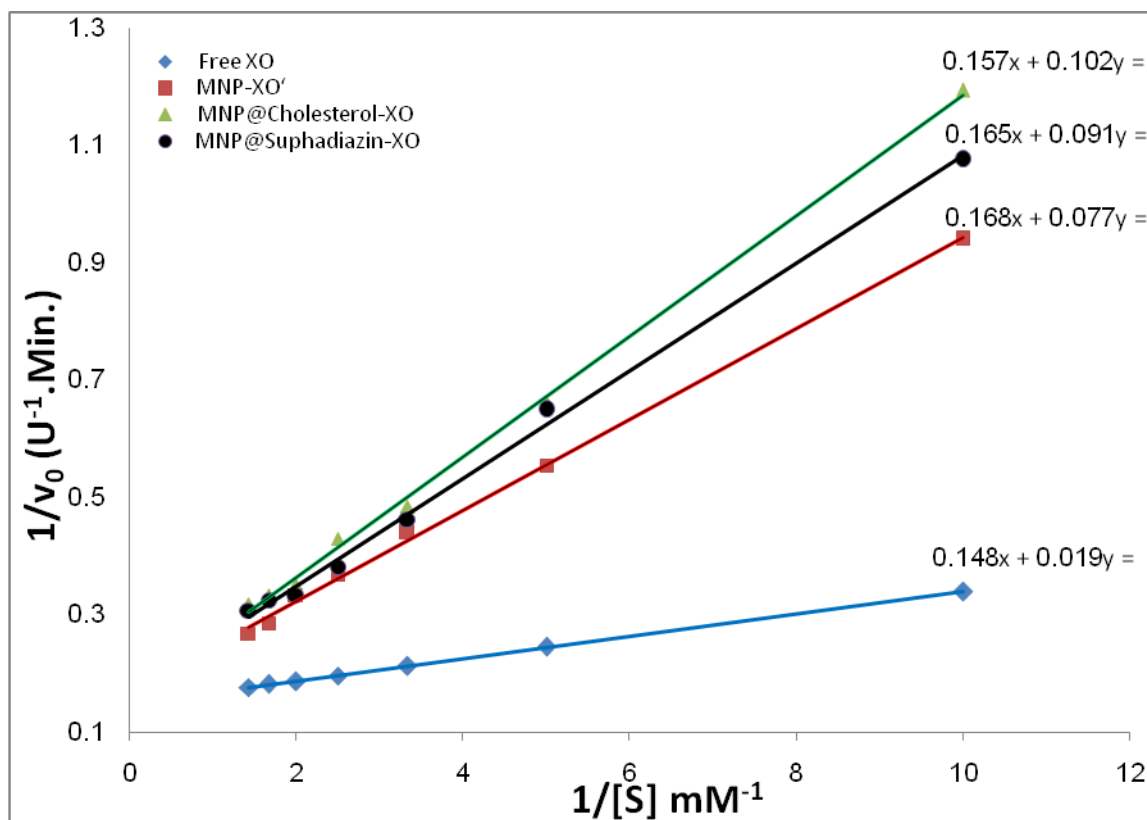


Figure 7. Lineweaver-Burke lines of the Free XO and XO immobilized on MNPs, MNP@Cholesterol, and MNP@Sulphadiazine

Binding of proteins on planar surfaces often induces significant changes in the secondary structure, but the high curvature of NPs aids proteins in retaining their original structure. However, a study of a variety of nanoparticle surfaces and proteins indicates that perturbation of protein structure still occurs to varying extents. The proteins show a rapid conformational change at both secondary and tertiary structure levels [39,40]. The structure and composition of the protein corona depends on the shape, composition, size, surface charges, and surface functional groups of the nanomaterial. Furthermore, the nature of the physiological compartment e.g., blood, interstitial fluid, etc., and the duration of exposure affect the protein corona structure and composition which alters the biological identity of the original biomolecules [41].

4. Conclusions

Two new magnetic nanoparticles were prepared and identified; MNP@Cholesterol and MNP@Sulfadiazine. These new particles in addition to magnetic Fe₃O₄ have the ability to adsorb and immobilize xanthine oxidase efficiently for future medical applications. Desorption quantities of the XO's from the surface of NPs were low in general and the adsorption processes were exothermic.

References

- [1] Leong GJ, Ebnonnasir A, Schulze MC, Strand MB, Ngo C, Maloney D, Frisco SL, Dinh HN, Pivovar B, Gilmer GH, Kodambaka S, Ciobanu CV, Richards RM. Shape-directional growth of Pt and Pd nanoparticles. *Nanoscale*. 2014;6(19):11364-71.
- [2] Castillo PM, de la Mata M, Casula MF, Sánchez-Alcázar JA, Zaderenko AP. PEGylated versus non-PEGylated magnetic nanoparticles as camptothecin delivery system. *Beilstein J Nanotechnol*. 2014; 5: 1312-9.
- [3] Li D, Tang X, Pulli B, Lin C, Zhao P, Cheng J, Lv Z, Yuan X, Luo Q, Cai H, Ye M. Theranostic nanoparticles based on bioreducible polyethyleneimine-coated iron oxide for reduction-responsive gene delivery and magnetic resonance imaging. *Int J Nanomedicine*. 2014; 9: 3347-61.
- [4] Samanta A, Ravoo BJ. Magnetic Separation of Proteins by a Self-Assembled Supramolecular Ternary Complex. *Angew Chem Int Ed Engl*. 2014 Sep 22.
- [5] Kasten A, Grütner C, Kühn JP, Bader R, Pasold J, Frerich B. Comparative In Vitro Study on Magnetic Iron Oxide Nanoparticles for MRI Tracking of Adipose Tissue-Derived Progenitor Cells. *PLoS One*. 2014; 9(9): e108055.
- [6] Céspedes E, Byrne JM, Farrow N, Moise S, Coker VS, Bencsik M, Lloyd JR, Telling ND. Bacterially synthesized ferrite nanoparticles for magnetic hyperthermia applications. *Nanoscale*. 2014 Sep 18.
- [7] Kado, T. Structural and magnetic properties of magnetite-containing epitaxial iron oxide films grown on MgO(001) substrates. *Journal of Applied Physics*. 2008; 103(4), 043902-4.
- [8] Laurent S, Saei AA, Behzadi S, Panahifar A, Mahmoudi M. Superparamagnetic iron oxide nanoparticles for delivery of therapeutic agents: opportunities and challenges. *Expert Opin Drug Deliv*. 2014; 11(9): 1449-70.
- [9] Zhang ZJ, Ma J, Xu SB, Ren JH, Qin Y, Huang J, Yang KY, Zhang ZP, Wu G. Synthesis and characterization of surface-modified Fe₃O₄ super-paramagnetic nanoparticles. *J Huazhong Univ Sci Technol Med Sci*. 2014; 34(2): 270-5.
- [10] Treuel L¹, Eslahian KA, Docter D, Lang T, Zellner R, Nienhaus K, Nienhaus GU, Stauber RH, Maskos M. Physicochemical characterization of nanoparticles and their behavior in the biological environment. *Phys Chem Chem Phys*. 2014; 16(29): 15053-67.
- [11] Docter D, Bantz C, Westmeier D, Galla HJ, Wang Q, Kirkpatrick JC, Nielsen P, Maskos M, Stauber RH. The protein corona protects against size- and dose-dependent toxicity of amorphous silica nanoparticles. *Beilstein J Nanotechnol*. 2014; 5: 1380-92.

- [12] Cedervall T, Lynch I, Lindman S, Berggard T, Thulin E, et al. Understanding the nanoparticle-protein corona using methods to quantify exchange rates and affinities of proteins for nanoparticles. *Proc Natl Acad Sci USA*. 2007; 16: 2050-2055.
- [13] Mu X, Qiao J, Qi L, Liu Y, Ma H. Construction of a D-amino acid oxidase reactor based on magnetic nanoparticles modified by a reactive polymer and its application in screening enzyme inhibitors. *ACS Appl Mater Interfaces*. 2014; 6(15): 12979-87.
- [14] Masuoka, N.; Nihei, K.; Maeta, A.; Yamagiwa, Y.; Kubo, I. Inhibitory effects of cardols and related compounds on superoxide anion generation by xanthine oxidase. *Food Chem*. 2014; 166: 270-274.
- [15] Kumar D, Kaur G, Negi A, Kumar S, Singh S, Kumar R. Synthesis and xanthine oxidase inhibitory activity of 5,6-dihydropyrazolo/pyrazolo[1,5-c]quinazoline derivatives. *Bioorg Chem*. 2014; 57C: 57-64.
- [16] Guan Q, Cheng Z, Ma X, Wang L, Feng D, Cui Y, Bao K, Wu L, Zhang W. Synthesis and bioevaluation of 2-phenyl-4-methyl-1,3-selenazole-5-carboxylic acids as potent xanthine oxidase inhibitors. *Eur J Med Chem*. 2014; 85: 508-16.
- [17] Zhang Z, Zhang Y, Method of calculating the thermodynamic parameters from some isothermal absorption models. *J. Acta of Northwest Sci-Tech Univ Agric Forestry*. 1998, 26(2): 94-98.
- [18] Kalckar H.M.. Differential spectrophotometry of purine compounds by means of specific enzymes; determination of hydroxypurine compounds. *The Journal of biological chemistry*. 1947; 167(2): 429-443.
- [19] Bradford, M.M. "Rapid and sensitive method for the quantitation of microgram quantities of protein utilizing the principle of protein-dye binding", *Anal. Biochem*. 1976; 72: 248-254.
- [20] You Q, Antony J, Sharma A, Nutting J, Sikes D, Meyer D. Iron/iron oxide core-shell nanoclusters for biomedical applications. *J Nanopart Res*. 2006; 8: 489-496.
- [21] Silva VAJ, Andrade PL, Silva MPC, Bustamante A, Valladares LDS, Aguiar JA. Synthesis and characterization of Fe₃O₄ nanoparticles coated with fucan polysaccharides. *J Magn Magn Mater*. 2013; 343: 138-143.
- [22] Conde J, Dias JT, Grazi V, Moros M, Baptista PV, de la Fuente JM. Revisiting 30 years of biofunctionalization and surface chemistry of inorganic nanoparticles for nanomedicine. *Front Chem*. 2014; 2: 48.
- [23] Behzadi S, Serpooshan V, Sakhtianchi R, Müller B, Landfester K, Crespy D, Mahmoudi M. Protein corona change the drug release profile of nanocarriers: The "overlooked" factor at the nanobio interface. *Colloids Surf B Biointerfaces*. 2014; pii: S0927-7765(14)00477-9.
- [24] Sobczynski DJ, Charoenphol P, Heslinga MJ, Onyskiw PJ, Namdee K, Thompson AJ, Eniola-Adefeso O. Plasma protein corona modulates the vascular wall interaction of drug carriers in a material and donor specific manner. *PLoS One*. 2014; 9(9): e107408.
- [25] Aili, D., Enander, K., Rydberg, J., Nesterenko, I., Bjorefors, F., Baltzer, L., Liedberg B. Folding induced assembly of polypeptide decorated gold nanoparticles. *J Am Chem Soc*. 2008; 130: 5780-5788.
- [26] De M, Rana S, Rotello VM. Nickel-ion-mediated control of the stoichiometry of His-tagged protein/nanoparticle interactions. *Macromol Biosci* 2009, 9: 174-178.
- [27] Arroyo-Maya JJ, Hernández-Sánchez H, Jiménez-Cruz E, Camarillo-Cadena M, Hernández-Arana A. α -Lactalbumin nanoparticles prepared by desolvation and cross-linking: Structure and stability of the assembled protein. *Biophys Chem*. 2014; 193-194: 27-34.
- [28] Perez-Iratxeta C, Andrade-Navarro MA. K2D2: estimation of protein secondary structure from circular dichroism spectra. *BMC Structural Biology*. 2008; 13;8:25. doi: 10.1186/1472-6807-8-25.
- [29] Seehuber A, Dahint R. Conformation and activity of glucose oxidase on homogeneously coated and nanostructured surfaces. *J Phys Chem B*. 2013; 117(23): 6980-9.
- [30] Carter EL, Tronrud DE, Taber SR, Karplus PA, Hausinger RP. Iron-containing urease in a pathogenic bacterium. *Proc Natl Acad Sci USA*. 2011; 108: 13095-13099.
- [31] Caputo GA, London E. Cumulative effects of amino acid substitutions and hydrophobic mismatch upon the transmembrane stability and conformation of hydrophobic alpha-helices. *Biochemistry*. 2003; 42, 3275-85.
- [32] Lakowicz, J. R., In *Principles of Fluorescence Spectroscopy*, Kluwer-Plenum, NY, 1999.
- [33] Toth J. Adsorption: theory, modeling, and analysis *Surfactant, Marcel Dekker, Sci. Ser.* 2002; 107(50): 971-983.
- [34] Wang B, Peng W, Yokel RA, Eric A. Influence of surface charge on lysozyme adsorption to ceria nanoparticles. *App Surf Sci*. 2012; 258(14): 5332-5341.
- [35] Fischer N, Verma A, Goodman C, Simard J, Rotello V, Reversible "irreversible" inhibition of chymotrypsin using nanoparticle receptors. *J Am Chem Soc* 2003; 125:13387-13391.
- [36] Fei L, Perrett S. Effect of Nanoparticles on Protein Folding and Fibrillogenesis. *Int J Mol Sci*. 2009; 10: 646-655.
- [37] Rabe M, Verdes D, Seeger S. Understanding protein adsorption phenomena at solid surfaces. *Adv Coll Interface Sci*. 2011; 162(1-2): 87-106.
- [38] Case DA, Cheatham T, Darden T, Gohlke H, Luo R, Merz Jr KM, Onufriev A, Simmerling C, Wang B, Woods R: The Amber biomolecular simulation programs. *J Comput Chem*. 2005; 26: 1668-1688.
- [39] Shang W, Nuffer J, Dordick J, Siegel R. Unfolding of ribonuclease A on silica nanoparticle surfaces. *NanoLett*, 2007; 7: 1991-1995.
- [40] Wu SC, Lia YK Application of bacterial cellulose pellets in enzyme immobilization. *J Mol Catal B-Enzym*. 2008; 54: 103-108.
- [41] Walkey CD, Chan WC. Understanding and controlling the interaction of nanomaterials with proteins in a physiological environment. *Chem Soc Rev*. 2012; 41(7): 2780-99.